Self-generated randomness, defect wandering, and viscous flow in stripe glasses

Harry Westfahl, Jr.,[1] Jörg Schmalian,[1] and Peter G. Wolynes[2]
[1]*Department of Physics and Astronomy and Ames Laboratory, Iowa State University, Ames, Iowa 50011*
[2]*Department of Chemistry and Biochemistry, University of California, San Diego, La Jolla, California 92093*
(Received 15 February 2001; published 4 October 2001)

We show that the competition between interactions on different length scales, as relevant for the formation of stripes in doped Mott insulators, can cause a glass transition in a system with no explicitly quenched disorder. We analytically determine a universal criterion for the emergence of an exponentially large number of metastable configurations that leads to a finite configurational entropy and a landscape dominated viscous flow. We demonstrate that glassiness is unambiguously tied to a new length scale which characterizes the typical length over which defects and imperfections in the stripe pattern are allowed to wander over long times.

DOI: 10.1103/PhysRevB.64.174203 PACS number(s): 61.43.Gt, 75.10.Nr, 74.25.−q

I. INTRODUCTION

The competition of interactions on different length scales is one of the mechanisms able to stabilize mesoscale phase separations and create spatial inhomogeneities in a wide variety of systems. The most typical situation is a competition between short-ranged forces that favors the formation of a uniform condensed phase and the long-range forces which can energetically frustrate this condensation. Classical examples are the formation of domains in magnetic multilayer compounds[1,2] and mesoscopic structures built by assembling polymers in solution or amphiphiles in water-oil mixtures.[3,4] Very often, these systems exhibit a long-time dynamics similar to the relaxation seen in glasses. Conversely, many proposals have been made that the glassy behavior of molecular liquids might arise from frustration of specific crystallinelike orders incompatible with global packing, e.g., icosahedral order in dense liquids.[5]

The observation of complex orbital and charge patterns in colossal magnetoresistance (CMR) manganites or of charge stripes in doped nickelates and cuprates[6,7] suggests that a similar competition causes inhomogeneous structures in these strongly correlated electron systems.[8] This point of view is supported by the observation of spatial inhomogeneities[9–15] as well as slow, activated glassy dynamics,[12,14] as seen in recent NMR experiments. Upon cooling, the Cu NMR signal in $La_{2-x}Sr_xCuO_4$-based systems disappears (is ''wiped out''). This has been interpreted in terms of an electronic relaxation slower than the Larmor precession of the nuclear spins.[12,14] As a result, the NMR signal decays so fast that it simply cannot be detected anymore. Thus the ''wipe out effect'' discussed in Refs. 9–15 is clear evidence for a dramatic increase of the relaxation times of the electronic system. Similarly, La NMR was used to directly show that there is a glassy-activated dynamics with a maximum of $T_1^{-1}(T)$, separating relaxational dynamics which is slower than the nuclear Lamor frequency at low temperatures from faster processes at higher T.[12,14] The typical activation energies of these dynamical processes have been analyzed by Curro *et al.*[14] who made the surprising observation that they are rather independent of the specific details of added impurities, etc. Also, the width of the distribution of activation energies is comparable to its mean value in systems with rather different chemical composition. In view of this striking universality of the anomalous long-time relaxation in doped Mott insulators, we recently suggested that glassiness in these systems is *self-generated*; i.e., it does not rely on the presence of quenched disorder.[16,17] The latter may, in general, further stabilize a glassy state. This is supported by molecular dynamics calculations for charge ordering in transition metal oxides, which found an anomalous long-time relaxation with a power spectrum similar to $1/f$ noise.[18] In addition, recently Markiewicz *et al.*[19] analyzed neutron diffraction,[20] nuclear quadrupole resonance (NQR),[21] muon spin resonance (μSR),[22] anelastic relaxation,[21] and susceptibility measurements,[23] spanning altogether more than ten orders of magnitude of frequency, and also find a ''universal'' behavior of the activation energies in underdoped cuprates. They also find a good description of the relaxational dynamics using a Vogel-Fulcher law which we predicted based on an entropic droplet argument.[16]

In Refs. 16 and 17 we showed that the competition between interactions on different length scales causes the emergence of an exponentially large number of metastable states (with the system size). This is generally considered as a condition for the anomalous dynamical features of glassiness, like aging, memory effects, and ergodicity breaking. It is also the heart of the *random first-order transition* scenario[24] for vitrification of molecular liquids, originally motivated by the similarities between density functional theories of aperiodic crystals[25] and the mean-field theories for random spin glasses. This scenario is now believed to apply to a much more general class of systems. Our result was obtained using a replica approach[26,27] and by solving the resulting many-body problem numerically within the self-consistent screening approximation. In this paper we develop an analytical approach which enables us to identify the underlying physical mechanism for glassiness in a uniformly frustrated system. We furthermore discuss that our results can also be obtained within a dynamical approach, where glassiness is associated with an unconventional long-time limit of the charge correlation function.

In the next section we introduce the model we investigate and summarize the main results of this paper. The details of our approach are presented in Sec. IV, subsequent to our summary of the aspects of the stripe liquid state that will be

important for our results in Sec. III. In Sec. V we conclude and give a list of further open questions.

II. MODEL AND OVERVIEW

This paper develops an analytical approach to glassiness in a uniformly frustrated system. By uniformly frustrated we mean that there is a competition of interactions on different length scales and there are no explicitly quenched degrees of freedom, like the ones caused by additional defects or imperfections. We study a model with a local tendency towards phase separation, frustrated by a long-range interaction, which, as we will show, has all necessary features to exhibit a glass transition and yet is simple enough to be treated analytically. In the context of cuprate systems the model has been proposed by Emery and Kivelson[8] and is defined by the Hamiltonian

$$\mathcal{H}=\frac{1}{2}\int d^dx\left\{r_0\varphi(\mathbf{x})^2+[\nabla\varphi(\mathbf{x})]^2+\frac{u}{2}\varphi(\mathbf{x})^4\right\}+\frac{Q}{8\pi}\int d^dx\int d^dx'\frac{\varphi(\mathbf{x})\varphi(\mathbf{x}')}{|\mathbf{x}-\mathbf{x}'|}. \quad (1)$$

Here, $\varphi(\mathbf{x})$ characterizes charge degrees of freedom, with $\varphi(\mathbf{x})>0$ in a hole-rich region, $\varphi(\mathbf{x})<0$ in a hole-poor region, and $\varphi(\mathbf{x})=0$, if the local density equals the averaged one. If $r_0<0$, the system tends to phase separate since we have to guarantee charge neutrality $\langle\varphi\rangle=0$. The coupling constant Q is a measure for the frustration between this short-range coupling and the long-range Coulomb interaction. For $Q=0$ and $r_0<0$ we expect at low temperatures long-range charge ordering. The ordering temperature can be estimated within $N\to\infty$ approximation [where $\varphi($**x** is generalized to an N-component field)] as $T_c^0=2\pi^2|r_0|/u\Lambda$, with momentum cutoff Λ of the order of an inverse lattice constant. As shown in Ref. 28, within a large-N approach, for all $Q>0$, the Coulomb interaction suppresses this ordered state at finite T. Instead, as revealed by a mean-field analysis of Eq. (1) where $N\to\infty$, the system undergoes several crossovers.

As can be seen in Fig. 1, at high T two characteristic length scales occur. One is the charge ordering correlation length ξ, and the other $l_D\sim\xi^{-1}Q^{-1/2}$ is the effective Debye screening length of charged regions of size ξ (see Appendix C). Here we can already recognize the effect of the competition between the short-range ordering interaction and the long-range Coulomb interaction: the charge density is homogeneous within regions of size ξ, but behaves like a plasma with screening length $l_D\gg\xi$ on larger scales. In Ref. 29 it was argued that the emergence of the screening length l_D supports the formation of compact ordered domains of size l_D which then give rise to a slow motion and thus glassiness. How such Debye screening should cause such compact domains and glassiness has not been made explicit, however. Our replica approach gives no indication for glassiness in the temperature regime where the Debye screening theory applies. Thus, despite using the same Hamiltonian, the stripe glass phase discussed in this paper is qualitatively different from the scenario of Ref. 29. A more detailed discussion of these aspects is given in Appendix C.

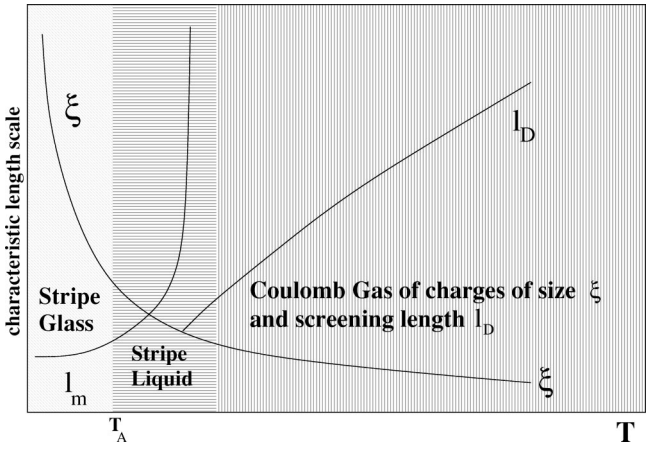

FIG. 1. The competition between different length scales according to the mean-field solution of Eq. (1).

As the temperature is lowered, ξ increases monotonically while l_D decreases until it becomes of the order of ξ. At this point, the Debye screening approximation breaks down and the system crosses over to a new regime characterized by spatial charge modulations, called stripes, with period $l_m\simeq 2\pi Q^{-1/4}$ and coherence length ξ[28]. These modulations are particularly relevant at low temperatures where the correlation length ξ is larger than the interstripe distance l_m and, as we will show, where the *stripe glass* phase emerges.

The charge correlation function $\mathcal{G}(\mathbf{x},\mathbf{x}')=T^{-1}\langle\varphi(\mathbf{x})\varphi(\mathbf{x}')\rangle$ of the liquid state at low temperatures is then characterized by two length scales l_m and ξ. After transformation into momentum space, this function obeys the following scaling behavior (neglecting effects due to anomalous powers):

$$\mathcal{G}(\mathbf{q})=l_m^2 g(ql_m, l_m/\xi), \quad (2)$$

with $\mathcal{G}(\mathbf{q})$ peaked at the modulation wave vector $q_m=2\pi/l_m$ with broadening ξ^{-1}. In thermodynamic equilibrium, the model, Eq. (1), undergoes a stripe-liquid–stripe-solid transition at some temperature T_c. Within a spherical approximation[30] or a large-N approximation,[28] the transition is of second order and $T_c\to 0$ [unless one takes additional lattice corrections into account which yield a finite T_c (Ref. 28). In the Ising limit ($N=1$), $T_c>0$ and there are indications that the transition is driven first order by fluctuations.[31]

Our results indicate that this phase transition may not be reached kinematically, in which case the system undergoes a glass transition instead. In fact, according to our theory, glassiness emerges if the interstripe correlations in the stripe liquid phase are sufficiently strong, specifically if the ratio ξ/l_m is larger than a critical value which we find to be close to 2. The temperature T_A where this happens, within the large-N approximation of Eq. (1), is given by

$$T_A = \frac{T_c^0}{\pi^2 Q^{1/4} + 1}, \tag{3}$$

which decreases for increasing frustration parameter Q.

Note that the criterion $\xi/l_m \simeq 2$ for glassiness is likely to be much more general than the specific formula for T_A, which depends on details of the model. Also, in a more realistic model, the stripe-liquid–stripe-solid transition, is expected to be of first order due to an additional term $\sim\varphi^3$ in Eq. (1) which exists if particle hole symmetry is broken. Nevertheless, our results do not depend on an actual divergence of ξ but solely that it is larger than a few interstripe separations. Therefore, our theory also applies if the transition is only moderately first order and the stripe solid does not occur unless $\xi > 2l_m$. In this case, the equilibrium transition is avoided and a glassy state results.

Our theory yields that below T_A the system establishes an exponentially large number of metastable states and long-time correlations, characterized by the correlation function $\mathcal{F}(\mathbf{x},\mathbf{x}') = T^{-1}\lim_{t\to\infty}\langle \phi(\mathbf{x},t)\phi(\mathbf{x}',0)\rangle$. These long-time correlations occur even though no state with actual long-range order exists. Even more interestingly, long-time correlations with $\mathcal{F}(\mathbf{x},\mathbf{x}') \neq 0$ are unambiguously tied to a new length scale λ, which characterizes the typical length over which defects and imperfections in the stripe pattern are allowed to wander over long times. This length can be associated with the allowed vibrational motions in a potential minima of the complex energy landscape of the system. In analogy with structural glasses we therefore call it the Lindemann length of the stripe glass.

Evidently, in the liquid state λ is infinite. In the glassy state we find that λ jumps discontinuously to a finite value $\lambda_A \simeq \xi(T_A)/3$ and continuously decreases at lower temperature. The discontinuous jump in λ, unaccompanied by a latent heat, indicates that the transition is of the random first-order type,[24] i.e., has one-step replica symmetry breaking. Thus, the glassy state is stable only if the slow motion of glassy textures is confined to a range smaller than λ_A (justifying our term Lindemann length). Due to this additional length scale, the following scaling behavior of the long-time correlations results:

$$\mathcal{F}(\mathbf{q}) = l_m^2 j\left(q l_m, \frac{l_m}{\xi}, \frac{l_m}{\lambda}\right), \tag{4}$$

with $j(x,y,z) = g(x,y) - g(x,\sqrt{z^2-y^2})$ and g from Eq. (2).

In Fig. 2 we show the momentum dependence of $\mathcal{F}(\mathbf{q})$ in comparison with $\mathcal{G}(\mathbf{q})$. Close to $q_m \equiv 2\pi/l_m$ (if $||\mathbf{q}| - q_m| \leqslant \xi^{-1}$) we have $\mathcal{F}(\mathbf{q}) \sim \mathcal{G}(\mathbf{q})$. Configurations which are close to perfect stripe arrangements are solely characterized by a momentum-independent Debye-Waller factor, such that

$$\mathcal{F}(\mathbf{q}) \simeq \frac{1}{1 + (\lambda/\xi)^2}\mathcal{G}(\mathbf{q}).$$

On the other hand, if $||\mathbf{q}| - q_m| \gtrsim \lambda^{-1}$, long-time correlations are much reduced compared to instantaneous correlations with $\mathcal{F}(\mathbf{q}) \simeq \lambda^{-2}\mathcal{G}(\mathbf{q})^2$. These "tails" of the correlation functions are obviously built up by configurations with defects and imperfections of the perfect stripe arrangement. Therefore, λ has to be interpreted as the length scale over which defects of the stripe pattern are allowed to wander after a long time. The glassy state can only be supported if $\lambda < \lambda_A$; it melts if defects are allowed to wander too far.

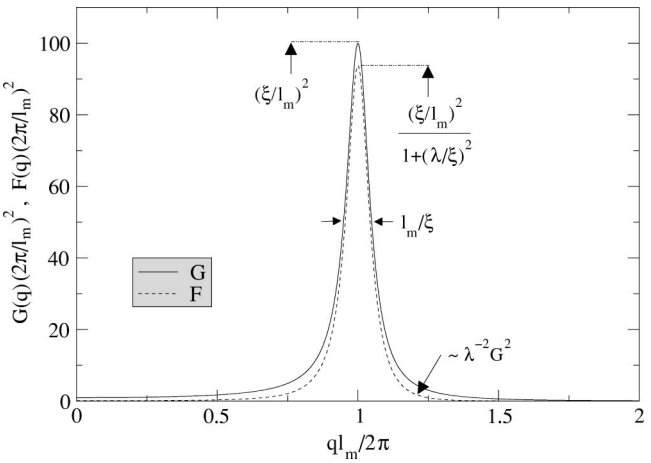

FIG. 2. The $\mathcal{G}$ and $\mathcal{F}$ correlation functions as given by Eqs. (2) and (4) for $l_m/\xi = \pi/10$ and $l_m/\lambda = 2\pi/5$.

Glassiness, including a viscous, energy-landscape-dominated long-time relaxation, sets in due to the occurrence of exponentially many metastable states $\mathcal{N}_{ms} \propto \exp(S_c)$.[24] We find that the configurational entropy

$$S_c(T_A) \sim Q^{3/4}V \sim l_m^{-3}V, \tag{5}$$

where V is the volume of the system. The shorter the modulation length, the larger is the number of possible metastable states, which is plausible for simple geometrical reasons. This clearly demonstrates that locally the stripe correlations stay intact in all these configurations. Furthermore, it is the packing of stripes with different orientation and the arrangement of defects that distinguishes the many different metastable states.

In the laboratory, the system will freeze into a glass, at some temperature $T_G < T_A$ which depends on the cooling rate. While this glass transition is purely dynamical and distinct from a conventional phase transition, a key feature of the ideal glass transition scenario of Ref. 24 is that the slowing arises from proximity to an underlying random first-order transition at $T_K < T_G$, where the configurational entropy vanishes like $S_c(T) \propto T - T_K$. Our theory gives exactly this behavior with

$$S_c(T) = l_m^{-3}\Psi(\lambda/\xi, l_m/\xi)V.$$

We find $\Psi(s,t) = (1+s^{-1})(1-t)^2 + \ln[1-(1-t)^2]$ which vanishes linearly at a temperature T_K. Below T_K the system freezes into an amorphous solid state due to this "entropy crisis,"[32] even for an infinitely slow cooling rate. Usually, the reason for the system to prefer the liquid state over the solid is entropic. If $S_c \to 0$, there is no entropic advantage anymore to be in the liquid state and the amorphous solid results, even in equilibrium.

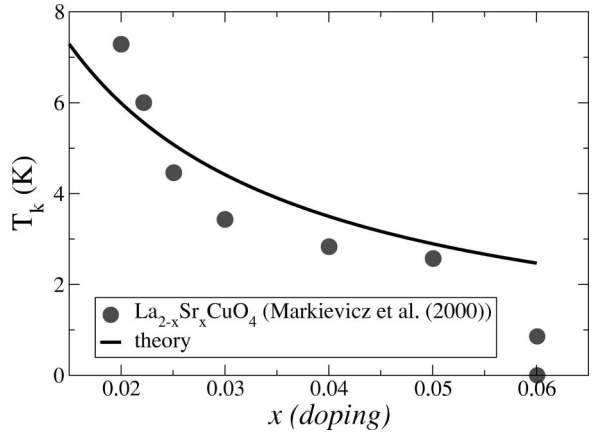

FIG. 3. Comparison of T_K with the experimental data analyzed by Markiewicz *et al.* (Ref. 19).

Freezing into a glassy state below T_A implies that within our replica approach the barriers between different metastable states are infinite. This, however, is a consequence of the mean-field character of the replica technique. Following Ref. 24 we argue that the formation of a mosaic pattern with dynamically defined droplets of size R of different metastable states will occur. Entropy-driven transitions between different states lead to dynamical processes with relaxation time obeying a Vogel-Fulcher law

$$\tau \propto \exp\left(\frac{DT_K}{T-T_K}\right), \tag{6}$$

with fragility

$$D(Q) \propto \frac{\sigma_0^2(Q)}{\left.\frac{dS_c(Q,T)}{dT}\right|_{T_K}} \tag{7}$$

determined by the configurational entropy as well as the bare surface tension of entropic droplets $\sigma_0(Q)$. Finally, a simple estimate for σ_0, based on a variational argument, gives $D(Q) \propto \sqrt{Q}$ to a good approximation. This was recently found in numerical simulations of the lattice version of Eq. (1) by Grousson *et al.*[33]

Recently, Markiewicz *et al.*[19] analyzed various experiments performed on $La_{2-x}Sr_xCuO_4$, spanning altogether 13 orders of magnitude of frequency, and also found a ''universal'' behavior of the activation energies in underdoped cuprates. Interestingly, a good description of the relaxational dynamics using a Vogel-Fulcher law, Eq. (6), is possible. The analysis of Ref. 19 also yields that T_K decreases with increasing doping concentration x. Using the relation, $l_m \simeq a(2x)^{-1}$,[34] between interstripe distance l_m and the doping concentration (with a being the lattice spacing), as well as $l_m \simeq 2\pi Q^{-1/4}$, enables us to determine the doping dependence of T_K and show that it is properly described within our theory. This is shown in Fig. 3 in comparison with the results as deduced from experiment in Ref. 19. Indeed, our theory gives the proper doping dependence of T_K. If we neglect the differences between T_K and T_A (see inset of Fig. 5 below), an approximate formula for the doping dependence of T_K is $T_K \simeq T_c^0/(4\pi^3 x+1)$. The typical doping concentration on which changes in the glass transition temperature occur is $x_0 = 1/4\pi^3 \simeq 0.008$. Note that the experiments analyzed in Ref. 19 are solely sensitive to the spin excitations of the system. We argue that due to strong coupling between charge and spin degrees of freedom (which is evident from the formation of phase or antiphase domain walls), glassiness of the charge density causes the observed anomalous long-time dynamics in the spin channel. Note that due to parameters like u or r_0 which are not known quantitatively without starting from a more microscopic theory, we cannot determine the absolute magnitude of the freezing temperature T_{K}. On the other hand, the doping dependence of T_{K} should be fairly robust since it only depends on the interstripe distance. Similar to the number of metastable states, which is only determined by the way one can geometrically arrange different stripe pattern, is the Q dependence of the freezing temperature dominated by these geometrical aspects. This should make the doping dependence of T_{K} for low doping concentration independent of microscopic details.

III. STRIPE LIQUID

In this section we summarize the main results for the stripe liquid state needed for our subsequent calculations in the glass state. We will mostly use results obtained within the leading contribution of a $1/N$ expansion. We calculate higher-$1/N$ corrections and show that they are small in the low-temperature regime discussed here. Note also that the numerical solution presented in Ref. 16 did take higher-$1/N$ corrections systematically into account. The agreement between the results of this section with these numerical results also supports the neglect of $1/N$ corrections for the stripe liquid state. The latter will become essential, however, in the glass state.

The mean-field equations of the stripe liquid including $1/N$ corrections have been discussed in detail in Ref. 28. Some of these results have already been summarized above. In what follows we will mostly discuss the low-temperature regime where the correlation length ξ exceeds the modulation length l_m of the system. This means we will be concentrated in the high temperature region of Fig. 1.

In the mean-field approximation the correlation function is given by

$$\mathcal{G}(q) = \frac{1}{r+q^2+\dfrac{Q}{q^2}}, \tag{8}$$

where the parameter $r = r_0 + u\langle \phi^2 \rangle$ must be determined self-consistently. At high temperatures, $r > 2\sqrt{Q}$ and the system is characterized by a correlation length $\xi \sim r^{-1/2}$, similar to the unfrustrated system, as well as a Debye screening length $l_D \sim \xi^{-1} Q^{-1/2}$ characterizing conventional screening of charged objects with linear size ξ and charge $\sim Q^{1/2}$. In the limit $l_D \gg \xi$ the Fourier transform of $\mathcal{G}$ is given by

$$G(x)=\frac{e^{-x/\xi}-\left(\frac{\xi}{l_D}\right)^2 e^{-x/l_D}}{4\pi|x|}. \tag{9}$$

At lower temperatures, when $r(T)<2\sqrt{Q}$, simple Debye screening breaks down and the system establishes modulated structures with modulation length (interstripe distance) $l_m=4\pi/\sqrt{2\sqrt{Q}-r}$ and correlation length $\xi=2/\sqrt{r+2\sqrt{Q}}$.[28]

However, unless ξ becomes larger than l_m, no actual stripe correlations emerge. This happens only if, at even lower temperatures, the charge correlations are sufficiently strong to form a stripe liquid and different stripes are strongly correlated. We will focus on this temperature regime. Here, $0>r(T)>-2\sqrt{Q}$ and thus $G(x)$ exhibits an oscillatory behavior with $\xi>l_m$.

It will be useful to introduce the positive dimensionless parameter ε via

$$\varepsilon^2=\frac{4Q}{r^2}-1. \tag{10}$$

We then find (defining $q_m^2=-r/2\sim Q^{1/2}$ with $l_m=2\pi/q_m$) that one can approximate the correlation function as

$$\mathcal{G}(\mathbf{q})\simeq\frac{q_m^{-2}}{\left[\left(\frac{q}{q_m}\right)^2-1\right]^2+\varepsilon^2}. \tag{11}$$

In the last step we took only the leading term close to the peak at q_m into account. By doing this approximation we are breaking the charge neutrality condition $[\mathcal{G}(q=0)=0]$, only by a factor $\mathcal{G}(q=0)/\mathcal{G}(q_m)=\varepsilon^2$. For $\varepsilon\ll 1$, the leading contribution of the Fourier transform of $\mathcal{G}$ is given by

$$G(x)=\frac{e^{-x/\xi}\sin(2\pi x/l_m)}{4\pi\varepsilon|x|}, \tag{12}$$

which clearly shows the physical nature of the two length scales $\xi=2/\varepsilon q_m$ and $l_m=2\pi/q_m$. In order to have well-correlated stripes, the correlation length ξ must be much bigger than the modulation length l_m. This indeed translates into $\varepsilon\ll 1$ which can be used as a small parameter of the theory.

Within the large-N approximation, the temperature dependence of r is determined by

$$r=r_0+u_0T\int\frac{d^3p}{8\pi^3}\mathcal{G}(p). \tag{13}$$

For the case without frustration, $Q=0$, the usual critical temperature $T_c^0=2\pi^2|r_0|/u\Lambda$ results from the requirement $r(T_c^0)=0$. However, for finite Q no finite transition temperature occurs within the large-N approximation. Instead, one finds from Eq. (11) that

$$r(T)=r_0+\frac{u_0T}{2\pi^2}\left(\frac{\pi}{2}\frac{q_m}{\varepsilon}+\Lambda\right). \tag{14}$$

In Eq. (13) we ignored additional $1/N$ corrections, characterized by the self-energy at zero momentum. In the limit $\xi>l_m$ under consideration we find $\Sigma_G(0)\simeq-8q_m^2\varepsilon/\pi$. Since ε is small, the one-loop self-energy correction to G can be safely neglected, given that Σ_G is an additive correction to the second term on the right-hand side (RHS) of Eq. (14) which behaves, in leading order, as ε^{-1}. From Eqs. (10) and (14) we find at low temperatures

$$\varepsilon=\frac{\pi}{2}Q^{1/4}\frac{T/T_c^0}{\frac{2\sqrt{Q}}{r_0}+1-\frac{T}{T_c^0}}\simeq\frac{\pi}{2}Q^{1/4}\frac{T/T_c^0}{1-\frac{T}{T_c^0}}, \tag{15}$$

where in the last step $|r_0|\gg 2\sqrt{Q}$ was assumed. This relationship will be useful for the determination of the temperature T_A, where glassiness sets in.

IV. STRIPE GLASS

A. Spontaneous ergodicity breaking and replica formalism

With few exceptions,[35–38] the analytical investigation of glassiness due to the emergence of a large number of metastable states has concentrated on systems with quenched randomness. A major step forward was made in Refs. 26 and 27, where a new replica approach, equally applicable to quenched random and nonrandom systems, was developed. Within this approach, the configurational entropy for models of structural glasses was calculated, in good agreement with computer simulations.[27] Here, we use this approach to investigate the physics of self-generated stripe glasses.

The equilibrium's free energy density is given as $F=(-T/V)\ln Z$. It is of relevance only if the system is kinetically able to explore the entire phase space. Alternatively, one can introduce the averaged typical free energy of a system using the following recipe of an "ergodicity breaking field."[26,27]

Locally stable field configurations can be identified using a test field $\psi(\mathbf{r})$ and computing the partition sum

$$Z[\psi]=\int D\varphi\exp\left(-\mathcal{H}[\varphi]/T-\frac{g}{2}\int d^dx[\psi(\mathbf{x})-\varphi(\mathbf{x})]^2\right), \tag{16}$$

where $g>0$ denotes the strength of the coupling. Evidently, the free energy

$$\tilde{f}[\psi]=-T\ln Z[\psi] \tag{17}$$

will be small when the field ψ equals to a field configuration which locally minimizes $\mathcal{H}$. Thus, sampling all configurations of the ψ field, weighted with $\exp(-\beta\tilde{f}[\psi])$, is essentially a procedure to scan all locally stable configurations. The quantity

$$\tilde{F}=\lim_{g\to 0}\frac{1}{W}\int D\psi\tilde{f}[\psi]\exp(-\beta\tilde{f}[\psi]) \tag{18}$$

is the weighted average of the free energy density of all locally stable configurations. Here, $W=\int D\psi \exp(-\tilde{f}[\psi]/T)$ is introduced for proper normalization.

It is physically appealing then to introduce the free energy difference δF via

$$F=\tilde{F}-\delta F, \tag{19}$$

where δF gives the amount of energy lost if the system is trapped into locally stable states and hence not able to explore the entire phase space of the ideal thermodynamic equilibrium. If the limit $g\to 0$ on Eq. (18) behaves perturbatively, $\delta F=0$. This indicates that the number of locally stable configurations stays finite in the thermodynamic limit or at least grows less rapid than exponential with V. In this case all states are kinetically accessible. On the other hand, if the limit $g\to 0$ does not behave perturbatively, it means that the number of locally stable states, $\mathcal{N}_{\rm ms}$, is exponentially large in V. This allows us to identify the difference between the equilibrium and typical free energy as an entropy:

$$\delta F=TS_c. \tag{20}$$

The configurational entropy density $S_c=\ln \mathcal{N}_{\rm ms}$ is a measure of the number of metastable states and is an extensive quantity if there are exponentially many of those states. Its emergence renders the system incapable of exploring the entire phase space. S_c is then the amount of entropy which the system that freezes it into a glassy state loses due to its nonequilibrium dynamics.

In order to find an explicit expression for S_c one introduces a replicated free energy[26]

$$F(m)=-\lim_{g\to 0}\frac{T}{m}\ln\int D\,\psi Z[\psi]^m, \tag{21}$$

from which $\tilde{F}$ can be obtained as $\tilde{F}=\partial mF(m)/\partial m|_{m=1}$ and hence

$$S_c=\frac{1}{T}\left.\frac{\partial F(m)}{\partial m}\right|_{m=1}. \tag{22}$$

Inserting $Z[\psi]$ of Eq. (16) into Eq. (21) and integrating over ψ, one gets

$$F(m)=-\frac{T}{m}\ln Z(m), \tag{23}$$

with replicated partition function given by

$$Z(m)=\lim_{g\to 0}\int D^m\varphi \exp-\left(\sum_{a=1}^{m}\mathcal{H}[\varphi^a]/T - \frac{g}{2m}\sum_{a,b=1}^{m}\int d^dx\,\varphi^a(\mathbf{x})\varphi^b(\mathbf{x})\right), \tag{24}$$

which has a structure similar to a conventional equilibrium partition function. Note that, in the limit $g\to 0$, contributions proportional to g which are diagonal in the replica space can be safely neglected. The ergodicity breaking field ψ causes a coupling between replicas which might spontaneously lead to order in replica space even as $g\to 0$. This order is then associated with a finite S_c and thus glassiness.

Formally, Eq. (24) equals the partition function of system with quenched random field analyzed using the conventional replica approach. The main difference is that, here, the limit $m\to 1$ has to be taken. The resulting many-body problem in replica space is characterized by the matrix correlation function $\mathcal{G}_{ab}(\mathbf{q})=\langle\varphi^a(\mathbf{q})\varphi^b(-\mathbf{q})\rangle$ in replica space with Dyson equation

$$\mathcal{G}^{-1}(\mathbf{q})\Big|_{ab}=\mathcal{G}_0^{-1}(\mathbf{q})\,\delta_{ab}+\Sigma_{ab}(\mathbf{q})-\frac{g}{m}. \tag{25}$$

Here, $\mathcal{G}_0(\mathbf{q})$ is the Hartree propagator of Eq. (8) which we approximate at low temperatures by Eq. (11). $\Sigma_{ab}(\mathbf{q})$ is the self-energy in replica space. If we find that, as a consequence of the ergodicity breaking coupling constant g, $\Sigma_{ab}(\mathbf{q})$ has finite off-diagonal elements, we can conclude that there must be an energy landscape sensitive to the infinitesimal perturbation g, supporting a glassy dynamics. On the other hand, if $\Sigma_{ab}(\mathbf{q})$ is diagonal, conventional ergodic dynamics results and the system is in its liquid state or may build an ordered solid. As pointed out above, this strategy is similar to the investigation of symmetry breaking in conventional phase transitions where the off-diagonal elements of an appropriately defined matrix self-energy are associated with the order parameter of the transition (superconducting gap function or staggered magnetization in the case of a superconductor or antiferromagnet, respectively). However, it turns out that in the present case the off-diagonal elements of $\Sigma_{ab}(\mathbf{q})$ jump discontinuously from zero to a finite value and a linearized theory with $\Sigma_{ab}(\mathbf{q})(1-\delta_{ab})$ small (which determines the transition temperature in the case of continuous phase transitions) will only give the trivial solution with vanishing off-diagonal elements. A nonlinear theory for $\Sigma_{ab}(\mathbf{q})$ needs to be developed.

Since the attractive potential between different replicas is symmetric with respect to the replica index, we use the following ansatz for the Green's function:

$$\mathcal{G}_{ab}(\mathbf{q})=[\mathcal{G}(\mathbf{q})-\mathcal{F}(\mathbf{q})]\,\delta_{ab}+\mathcal{F}(\mathbf{q}), \tag{26}$$

i.e., with equal diagonal elements $\mathcal{G}(\mathbf{q})$ and equal off-diagonal elements $\mathcal{F}(\mathbf{q})$. Note that if one applies the present replica formalism to systems with quenched disorder, it turns out that the replica-symmetric ansatz, Eq. (26), is equivalent to one-step replica symmetry breaking in the conventional replica formalism.[26] The physical interpretation of $\mathcal{G}(\mathbf{r}-\mathbf{r}')=T^{-1}\langle\varphi(\mathbf{r})\varphi(\mathbf{r}')\rangle$ as thermodynamic (instantaneous) correlation function is straightforward. On the other hand, $\mathcal{F}(\mathbf{r}-\mathbf{r}')=T^{-1}\lim_{t\to\infty}\langle\varphi(\mathbf{r},t)\varphi(\mathbf{r}',0)\rangle$ can be interpreted as measuring long-time correlations. As shown in Appendix A, inserting the ansatz, Eq. (26), into Eq. (25) gives in the limit $m\to 1$

$$\mathcal{G}^{-1}(\mathbf{q})=\mathcal{G}_0^{-1}(\mathbf{q})+\Sigma_{\mathcal{G}}(\mathbf{q}) \tag{27}$$

for the diagonal elements and

$$\mathcal{F}(\mathbf{q}) = \frac{-\mathcal{G}^2(\mathbf{q})\Sigma_{\mathcal{F}}(\mathbf{q})}{1-\mathcal{G}(\mathbf{q})\Sigma_{\mathcal{F}}(\mathbf{q})}$$

$$= \mathcal{G}(\mathbf{q}) - \frac{1}{\mathcal{G}^{-1}(\mathbf{q})-\Sigma_{\mathcal{F}}(\mathbf{q})} \equiv \mathcal{G}(\mathbf{q}) - \mathcal{K}(\mathbf{q}) \quad (28)$$

for the off-diagonal elements, respectively. Here, $\Sigma_{\mathcal{G}}$ and $\Sigma_{\mathcal{F}}$ are the diagonal and off-diagonal elements of the self-energy in replica space. In the last equation $\mathcal{K}$ denotes the deviations of the long-time and instantaneous correlations. Analyzing the corresponding dynamical equations of the problem, it turns out that $\mathcal{K}$ is the static retarded response function.[39] In the liquid state fluctuation dissipation theorem gives $\mathcal{K}=\mathcal{G}$ and no long-time correlations occur.

B. Defect wandering in stripe glasses

The self-energy in replica space was numerically investigated in Ref. 16 within the self-consistent screening approximation which we summarize in Appendix A. It was shown that below a characteristic temperature T_A, an off-diagonal self-energy in replica space emerges, leading to finite long-time correlations $\mathcal{F}(\mathbf{q})$, as well as a finite configurational entropy density

$$s_c = S_c/V \quad (29)$$

in the thermodynamic limit $V\to\infty$. Here we present an approximate but analytical solution of the same set of equations which has the appeal that the underlying physics of the stripe glass formation becomes much more transparent. It also reveals more directly the emergence of a new length scale which characterizes the wandering of defects in the stripe pattern after long times. In this context, we demonstrate that the melting of the glass as T becomes larger than T_A is a consequence of the fact that the characteristic length for defect wandering becomes too large; the glass becomes too fluid, causing the devitrification into a stripe liquid.

The key assumption of the analytical approach to the self-consistent screening approximation is that the off-diagonal self-energy $\Sigma_{\mathcal{F}}(\mathbf{q})$ is weakly momentum dependent. Specifically, we assume that due to the strong momentum dependence of the correlation function, the product $\mathcal{G}(\mathbf{q})\Sigma_{\mathcal{F}}(\mathbf{q})$ varies with $\mathbf{q}$ predominantly due to $\mathcal{G}(\mathbf{q})$. This assumption will be justified *a posteriori*. Also, our numerical results, which were obtained without any restriction on the $\mathbf{q}$ dependence of $\Sigma_{\mathcal{F}}(\mathbf{q})$, clearly show that this assumption is justified. We will then calculate $\Sigma_{\mathcal{F}}(q_m)$ at the modulation wave vector q_m.

From the analysis of the liquid state we know that $\mathcal{G}(q)$ is strongly peaked at the modulation vector q_m with width ξ^{-1}. By inspection of the Dyson equation (28), for $\mathcal{F}$, one can see that for $q\sim q_m$ and $\Sigma_{\mathcal{F}}(q_m)\mathcal{G}(q_m)\gg 1$ (since $\mathcal{G}$ is peaked around $q=q_m$)

$$\mathcal{F}(q) \lesssim \mathcal{G}(q). \quad (30)$$

Moreover, $\mathcal{G}$ vanishes rapidly away from the peak [as does $\Sigma_F(q_m)G(q_m)$] and it follows from the same equation (28) that for large $|q-q_m|$

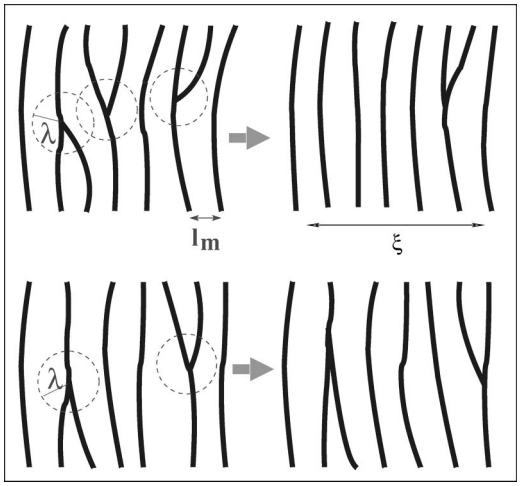

FIG. 4. Pictorial description of the wandering of defects in the stripe pattern. The upper panel shows defects that can be healed by the wandering process. The lower panel shows defects which are too far apart and cannot be healed.

$$\mathcal{F}(q) \simeq -\Sigma_{\mathcal{F}}(q)\mathcal{G}^2(q). \quad (31)$$

If a solution for $\mathcal{F}$ exists, it is going to be peaked at q_m, but smaller and narrower than $\mathcal{G}$. Consequently, if a stripe glass occurs, the long-time limit of the correlation function in not just a slightly rescaled version of the instantaneous correlation function, but it is multiplied by a q-dependent function that leads to a qualitatively different behavior for different momenta. Once a glassy state is formed, configurations which contribute to the peaks of $\mathcal{G}(q)$ and $\mathcal{F}(q)$, i.e., almost perfect stripe configurations, are almost unchanged even after long times. Close to q_m, $\mathcal{F}(q)$ is solely reduced by some momentum-independent Debye-Waller factor $\exp(-D)=\mathcal{F}(q)/\mathcal{G}(q)$. On the other hand, certain configurations which form the tails of $\mathcal{G}(q)$, i.e., defects and imperfections of the stripe pattern, disappear after a long time since now $\mathcal{F}(q)\ll\mathcal{G}(q)$. The ratio of both functions is now strongly momentum dependent. $\mathcal{F}(q)$ becomes sharper than $\mathcal{G}(q)$ because certain defects got healed in time. Evidently, there must be a momentum scale (or equivalently a length scale) which determines the transition between these two regimes. In what follows we will identify and determine this length scale. A pictorial description of the defects on the stripe configuration and the meaning of λ is presented in Fig. 4.

Due to our assumption that $\Sigma_{\mathcal{F}}$ is weakly dependent on q, we concentrate on $\Sigma_{\mathcal{F}}(q_m)$ at the modulation wave vector. One easily finds that $\Sigma_{\mathcal{F}}(q_m)\leqslant 0$. A dimensional analysis furthermore shows that $\Sigma_{\mathcal{F}}$ is length^{-2}. This suggests to define a new length scale λ via

$$\Sigma_{\mathcal{F}}(q_m) = -\left(\frac{2}{\lambda}\right)^2. \quad (32)$$

For the subsequent calculation it is convenient to introduce in addition to the dimensionless parameter ε which gives $\xi^{-1}=\varepsilon q_m/2$ a new dimensionless parameter κ, defined via

$$\lambda^{-1}=\frac{\sqrt{\kappa^2-\varepsilon^2}q_m}{2}. \tag{33}$$

Obviously, in the liquid state, where $\Sigma_{\mathcal{F}}\to 0$, we find $\lambda\to\infty$ and it holds $\kappa=\varepsilon$. In a glassy state $\kappa>\varepsilon$. This ansatz for $\Sigma_{\mathcal{F}}$, inserted into Eq. (28), yields

$$\mathcal{K}(q)=\frac{q_m^{-2}}{\left[\left(\frac{q}{q_m}\right)^2-1\right]^2+\kappa^2} \tag{34}$$

for the correlation function $\mathcal{K}=\mathcal{G}-\mathcal{F}$. Note that $\mathcal{K}$ has the same structure as $\mathcal{G}$ but with $\varepsilon\to\kappa$. It immediately follows that it is the length scale λ which determines whether long time correlations are similar or different from instantaneous ones. If $|q-q_m|<\lambda^{-1}$, Eq. (30) holds, whereas for $|q-q_m|>\lambda^{-1}$ long-time correlations are strongly reduced leading to Eq. (31). Consequently we identify λ as the length scale over which imperfections of the stripe pattern manage to wander; i.e., defects can be healed, even in the frozen glass state.

The next step is to determine $\Sigma_{\mathcal{F}}(q_m)$ for a given value of λ and to self-consistently determine this length scale. The details of the calculation of $\Sigma_{\mathcal{F}}(q_m)$ with $\mathcal{G}(q)$ as given in Eq. (11) and $\mathcal{K}(q)$ of Eq. (34) are summarized in Appendix B. The result is

$$\Sigma_{\mathcal{F}}(q_m)=-\frac{8q_m^2\varepsilon^2}{\pi}\frac{\left(1-\frac{\varepsilon}{\kappa}\right)^2}{1-\left(1-\frac{\varepsilon}{\kappa}\right)^2}\left(\frac{1}{\varepsilon}-\frac{1}{\kappa}\right). \tag{35}$$

This has to be compared with our ansatz, Eq. (32). Together with Eq. (33) this gives

$$\Sigma_{\mathcal{F}}(q_m)=-(\kappa^2-\varepsilon^2)q_m^2. \tag{36}$$

Comparing Eqs. (35) and (36) we immediately find the nonlinear algebraic equation

$$\kappa^2-\varepsilon^2=\frac{8\varepsilon^2}{\pi}\frac{\left(1-\frac{\varepsilon}{\kappa}\right)^2}{1-\left(1-\frac{\varepsilon}{\kappa}\right)^2}\left(\frac{1}{\varepsilon}-\frac{1}{\kappa}\right), \tag{37}$$

which determines the length scale λ (via κ), as a function of the correlation length and the modulation length, i.e., properties of the liquid state. One solution of this equation is always $\varepsilon=\kappa$, which corresponds to the liquid state. Factorizing this trivial solution from Eq. (37) we find that the other solutions are given by

$$\frac{\varepsilon}{\kappa}\left[\frac{8}{\pi\varepsilon}\left(1-\frac{\varepsilon}{\kappa}\right)^2-\left(1-\frac{\varepsilon}{\kappa}\right)\right]=2. \tag{38}$$

This is a cubic equation which can be solved exactly. Before we discuss this equation in some detail we analyze the condition for obtaining a nontrivial solution which corresponds to the onset of glassiness. For $8/\pi\varepsilon\gg 1$ the left-hand side of Eq. (38) has its maximum $1/\pi\varepsilon$ at $\kappa\simeq 3\varepsilon$ which gives the condition for the existence of a solution as $1/\pi\varepsilon\geqslant 2$. This defines the critical value of ε as

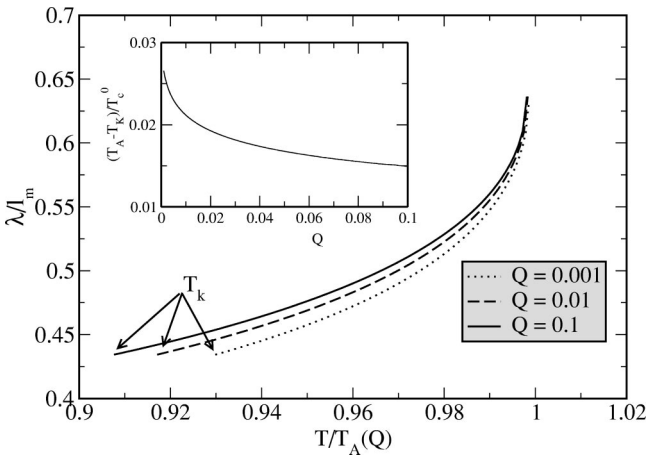

FIG. 5. The Lindeman length λ as a function of temperature for different values of Q. Inset: Q dependence of T_A-T_K, where T_K is obtained in Sec. IV D.

$$\varepsilon_A=\varepsilon(T_A)\simeq\frac{1}{2\pi}. \tag{39}$$

For $N>1$, it is straightforward to show that this result is generalized to $\varepsilon_A\simeq 1/2\pi N$. Thus, if the ratio of the correlation length and the modulation length exceeds the critical value

$$\left.\frac{\xi}{l_m}\right|_{T=T_A}\simeq 2, \tag{40}$$

long-time glassy correlations emerge. As expected, besides strong frustrations, glassiness also requires sufficiently strong liquid correlations. Since it follows from Eq. (38) that $\kappa\simeq 3\varepsilon$, it also follows that

$$\left.\frac{\lambda}{l_m}\right|_{T=T_A}\simeq\frac{2}{3}. \tag{41}$$

This type of behavior is evident in Fig. 5 where, independent of the value of Q, all curves for λ/l_m reach the same maximum value at T_A. If defects and imperfections of the stripe pattern within the glassy state manage to flow over length scales larger than $\simeq\frac{2}{3}l_m$, the glass becomes unstable because it is too fluid to support a frozen state. Thus, we identify the length scale λ as the Lindemann length of the glass.

As can be seen in Fig. 5, λ is a monotonically increasing function of temperature. At small temperatures λ grows linearly, evolving to a cusp at the dynamical freezing temperature T_A. Above T_A, λ becomes infinite and the devitrification is complete.

Using the Q dependence of ε in the liquid state [see Eq. (15)] the stripe-glass–stripe-liquid transition temperature is then given by

$$\varepsilon_A = \frac{1}{2\pi} = \frac{\pi}{2} Q^{1/4} \frac{T_A/T_c^0}{1 - \dfrac{T_A}{T_c^0}}, \tag{42}$$

which gives

$$T_A = \frac{T_c^0}{\pi^2 Q^{1/4} + 1}, \tag{43}$$

where T_c^0 is critical temperature of the $Q=0$ problem. Moreover, since the difference between T_A and T_K is small compared to T_c^0 (see the inset of Fig. 5), the Q dependence of T_K will be roughly the same as of T_A. As pointed out above, we do not expect T_A to be sensitively affected by an additional $(v/3)\varphi^3$ term in the Hamiltonian. This is less clear for the Kautzmann temperature (see Sec. IV D) and the difference between T_A and T_K might well depend on the coupling constant v. Still we expect T_K to decrease for increasing Q.

C. Lattice corrections

Until this point our theory has been performed in the continuum's limit and effects due to lattice corrections have been neglected. The particular form of the propagator, Eqs. (8) and (11), however, gives rise to a specific sensibility of our results to lattice corrections which is worth mentioning. Within the continuum's limit, the large-N approach used in this paper yields no ordinary phase transition to a stripe solid state, a result which has been pointed out earlier.[28,30] This can be most easily seen from the mean-field equation (14). A solution $\varepsilon = 0$ is only allowed if $T=0$. For $T>0$ one always finds a large, but finite correlation length, $\xi = 2/\varepsilon q_m$. The absence of an ordered state is a consequence of the dispersion relation ω_q, with

$$\omega_q = q_m \sqrt{\left[1 - \left(\frac{q}{q_m}\right)^2\right]^2 + \varepsilon^2}. \tag{44}$$

In contrast to an antiferromagnet or a conventional charge density wave, where the low-energy modes are determined by isolated points in momentum space, Eq. (44) gives rise to a $(d-1)$-dimensional sphere of low-energy modes in momentum space (see upper panel of Fig. 6). It is this large phase space of low-energy excitations which destroys long-range order.

The most dramatic effect of corrections beyond the continuum's limit is the appearance of an anisotropy on the low-energy states. It is reasonable to assume that the Hamiltonian (1) has a next-order correction of the type $4Kq_x^2 q_y^2$ which leads to a direction-dependent "mass" term in Eq. (44),

$$\varepsilon^2 = \varepsilon^2(K=0) + K q_m^2 \sin^2(2\phi), \tag{45}$$

with angle ϕ (in the x-y plane) and a dimensionless anisotropy parameter K. Of course this is only justified if $K \ll q_m^{-2}$. If, however, $K \simeq q_m^{-2}$, the physics strongly depends on phenomena on the scale of the interatomic spacing.

The mean-field equation for finite K is then given by

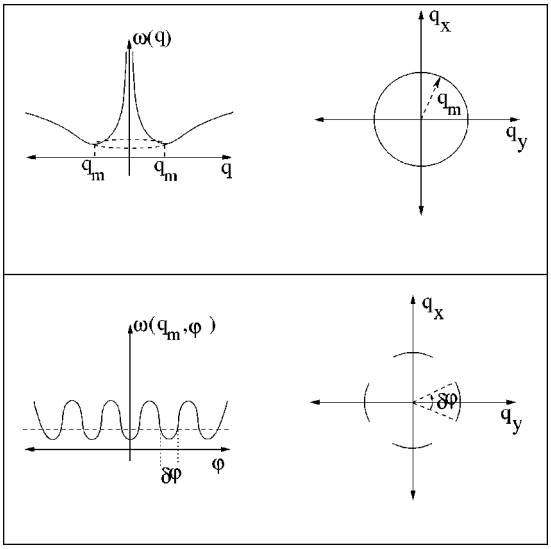

FIG. 6. Low-energy modes. Upper panel: in the continuum's limit, $K=0$, the phase space for low-energy excitations is a $d-1$ sphere. Lower panel: the anisotropy gives rise to a "direction-dependent mass" and the phase space for low-energy excitations is reduced to a set of arcs.

$$r(T) = r_0 + \frac{u_0 T}{2\pi^2}\left(\frac{\pi}{2}\frac{q_m}{\sqrt{\varepsilon(K=0)^2 + K q_m^2}} + 1\right). \tag{46}$$

The system now undergoes a phase transition for arbitrary small K at $T_c = T_c^0/(\pi K^{-1/2}\Lambda + 1)$. As expected, T_c vanishes as $K \to 0$. Moreover, as pointed out in Refs. 28 and 30, T_c does not merge with T_c^0 as $Q \to 0$. The origin of this phase transition is that the $(d-1)$-dimensional sphere of low-energy degrees of freedom is reduced to arcs of size $\delta\varphi \sim \varepsilon/(K^{1/2} q_m)$ (see lower panel of Fig. 6). As ε decreases, these arcs become indistinguishable from isolated points, a behavior similar to the case of an antiferromagnet or a charge density wave occurs, leading to an ordinary phase transition. The mean-field analysis of the lattice version of Eq. (3) of Ref. 30, which finds T_c considerably smaller than T_c^0 supports $K \ll q_m^{-2}$.

In analogy to the mean-field analysis of the liquid state one can also perform the theory of the glassy state for finite K. If lattice corrections are strong and $K \sim q_m^{-2}$, a transition to a stripe solid occurs at T_c. The low-energy excitations are located at isolated points and the behavior is equivalent to the one of an unfrustrated system. In this case, the glassy state will only occur if the solidification is avoided by supercooling. On the other hand, if $K \ll q_m^{-2}$, the low-energy modes are unchanged and the lattice corrections become irrelevant. Since the glass transition does not require ε to vanish, but solely to reach a certain finite limit $\sim 1/2\pi$, we conclude that for $K \lesssim q_m^{-2}/2\pi$ the glass transition is essentially unchanged.

D. Configurational entropy

The main argument for the emergence of a glassy state is the occurrence of an exponentially large number if meta-

stable states, characterized by the configurational entropy. S_c is determined from Eq. (22) from the replicated theory defined in Eq. (24), which gives $F(m)=(-T/m)\ln Z(m)$. Within the self-consistent screening approximation it follows that

$$F(m)/(2mT)=\mathrm{tr}\log\mathcal{G}^{-1}+\mathrm{tr}\ln\mathcal{D}^{-1}-\mathrm{tr}\,\Sigma\mathcal{G}.$$

Since all quantities are matrices in replica space with a structure given in Eq. (26), the evaluation of expressions like $\mathrm{tr}\ln\mathcal{G}^{-1}$, etc., becomes straightforward. Performing the derivative with respect to the number of replicas according to Eq. (22) gives immediately for the entropy density

$$s_c=s_c^{(1)}+s_c^{(2)},$$

with the two contributions

$$s_c^{(1)}=-\frac{1}{2}\int\frac{d^3q}{8\pi^3}\left\{\ln\left(1-\frac{\mathcal{F}(\mathbf{q})}{\mathcal{G}(\mathbf{q})}\right)+\frac{\mathcal{F}(\mathbf{q})}{\mathcal{G}(\mathbf{q})}\right\}$$

and

$$s_c^{(2)}=\frac{1}{2}\int\frac{d^3q}{8\pi^3}\left\{\ln\left(1-\frac{v_0\Pi_{\mathcal{F}}(\mathbf{q})}{1+v_0\Pi_{\mathcal{G}}(\mathbf{q})}\right)+\frac{v_0\Pi_{\mathcal{F}}(\mathbf{q})}{1+v_0\Pi_{\mathcal{G}}(\mathbf{q})}\right\}.$$

For the definition of $\Pi_{\mathcal{F}}$, $\Pi_{\mathcal{G}}$, etc., see Appendix A. Using the same approximations as for the evaluation of the self-energy, $\Sigma_{\mathcal{F}}$, in Appendix B we find

$$\frac{\mathcal{F}(\mathbf{q})}{\mathcal{G}(\mathbf{q})}\approx\frac{\kappa^2-\varepsilon^2}{\left[\left(\frac{q}{q_m}\right)^2-1\right]^2+\kappa^2}.$$

The evaluation of the integrals is straightforward and we find

$$s_c^{(1)}=\frac{q_m^3}{4\pi}\frac{\kappa}{2}\left(1-\frac{\varepsilon}{\kappa}\right)^2,$$

$$s_c^{(2)}=\frac{q_m^3}{4\pi}\frac{2}{\pi}\left\{\left(1-\frac{\varepsilon}{\kappa}\right)^2+\ln\left[1-\left(1-\frac{\varepsilon}{\kappa}\right)^2\right]\right\}. \qquad (47)$$

Obviously, $s_c\neq 0$ only if $\kappa>\varepsilon$; i.e., the Lindemann length λ is finite. s_c vanishes in the liquid state where $\kappa=\varepsilon$. The results for $s_c(T)$ for different values of Q are given in Fig. 7.

Using the results of the previous section where we found that for $T=T_A$ the dimensionless quantities ε and κ take fixed values, we obtain at $T=T_A$

$$S_c(T_A)=CVQ^{3/4}, \qquad (48)$$

with

$$C=\left(\frac{2}{\pi}+\frac{3}{4\pi}\right)\frac{1}{9\pi}+\frac{1}{2\pi^2}\ln\left(\frac{5}{9}\right)=1.1816\times10^{-3}.$$

The configurational entropy decreases for decreasing Q. Since the modulation length behaves as $l_m\sim Q^{1/3}$, it follows that $S_c\propto l_m^{-3}$. The larger the modulation length, the smaller is the number of states one can form, which clearly demonstrates that locally stripe correlations stay intact in all these configurations. It is more the packing and arrangement of defects which distinguish different metastable states. Fewer of those packings are possible per unit volume if the modulation length grows, for simple geometrical reasons. The relation (48) was recently derived by us using the concept of replica bound states.[17] The fact that we obtain the same result using an entirely different approach to solve the problem increases our confidence in the applicability of the self-consistent screening approximation, which also allows us to calculate the constant C. We can also compare $S_c(T_A)$ with the numerical results of Ref. 16. S_c was calculated in Ref. 16 for the values $Q=0.01$ and $Q=0.001$, where we found $S_c=3.45\times10^{-5}$ and 6.4×10^{-6}, respectively. From Eq. (48) we find the values 3.7×10^{-5} and 6.6×10^{-6}, which agrees well with the numerical results.

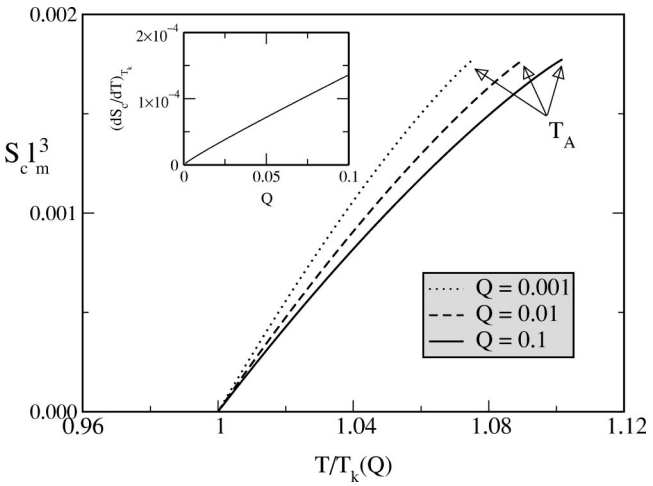

FIG. 7. The configurational entropy for different values of Q. Inset: dependence of $(dS_c/dT)_{T_k}$ on Q.

Finally, the condition $S_c(T=T_K)=0$ determines the Kauzmann temperature below which no entropic advantage of the liquid state, compared to the amorphous solid state (the glass) exists. Even if one manages to anneal the liquid down to T_K without freezing into a glass, something which might be achieved using an infinitely slow cooling rate, a mandatory transition into an amorphous solid occurs at T_K. In Fig. 7 we show the temperature dependence of S_c for different values of the frustration parameter Q as well as the Q dependence of the slope $(dS_c/dT)_{T_K}$.

E. Dynamics and flow via entropic droplet formation

So far, we have shown that within the self-consistent screening approximation of Eq. (1), an exponentially large number of metastable states occurs. The conclusion that somewhere below T_A nonequilibrium dynamic sets in is actually obtained using a purely thermodynamic characterization of the spectrum of metastable states. It is very plausible that an exponentially large number of metastable states is necessarily connected to glassy dynamics. In several random spin models as well as in the model of self-generated glassiness in frustrated Josephson junction arrays, this point of view has been clearly supported by actual dynamical calculations. For so-called infinite-range models (i.e., within

mean-field approximation), where the barriers between the various metastable states diverge, freezing at T_A has been found.[24,40]

Solving the Langevin equation for the time evolution of the correlation and response function of $\varphi(\mathbf{x},t)$, using the supersymmetric formulation of the Martin-Siggia-Rose approach[41] within the self-consistent screening approximation, we find that the emergence of exponentially many metastable states also leads to stripe glass state within a dynamical approach.[39] Interestingly, this mode-coupling-type approach gives exactly the same criterion for the emergence of glassiness as the above replica approach only if one properly takes the aging behavior of the dynamical evolution into account, following Ref. 42. Thus, the replica approach employed here takes the effects of aging correctly into account.

Within the mode coupling or replica integral equation approaches a perfect freezing occurs at the temperature T_A. However, more realistically, T_A is rather a crossover scale to a regime with slow activated dynamics and not the actual freezing temperature. Depending on the history of the system, the laboratory glass transition where the time scale of motions exceeds a certain limit occurs somewhere between T_K and T_A. A key question in this context is the nature of the dynamical processes for $T_K<T<T_A$.

This dynamics involves droplets or instantons, essential singularities from the point of view of perturbative approaches. A complete formal treatment is therefore difficult. Nevertheless, a reasonable description of the dynamics in a system with finite S_c is given in Ref. 24, where the nucleation of droplets with size R of a new state within an old one was argued to be the main dynamical processes. The free-energy gain of a droplet formation is caused by the entropic gain due to the exploration of new states, i.e., by Ts_cR^3, whereas one has to take into account that such a droplet implies a finite surface energy, characterized by a scale-dependent surface tension $\sigma(R)$. The energy landscape of these excitations should therefore be similar to the one of the random-field Ising model. The fundamental connection between this model and the replica approach used in this paper is also evident from Eq. (24). Thus we use a renormalization group calculation for the random-field Ising model, based on Ref. 43, which leads to the size-dependent surface tension

$$\sigma(R)=\sigma_0(R\Lambda)^{-\theta}. \tag{49}$$

Here $\theta=(d-2)/2$ reflects the fact that the interface between two states is wetted by intermediate states. This analysis leads to a characteristic energy barrier $\Delta E\propto[Ts_c(T)]^{-1}$ which implies a characteristic relaxation time which follows a Vogel-Fulcher law

$$\tau\propto\exp\left(\frac{DT_K}{T-T_K}\right), \tag{50}$$

independent of the dimension. Here, fragility parameter of the Vogel-Fulcher law is given by

$$D=\frac{3\sigma_0^2}{T^2T_K\left.\frac{dS_c}{dT}\right|_{T_K}}. \tag{51}$$

Xia and Wolynes[44] have shown that this scenario gives a quantitative description of viscous flow in molecular liquids A straightforward extension of Refs. 24 and 44 along the lines of Ref. 45 also gives a width of the distributions of different activation energies characterized by the mean-square width $\langle\delta R^2\rangle$ of the droplet size, which might be compared with the results of Ref. 14. This droplet picture implies that the glass breaks up into domains of different metastable states, separated by wetted surfaces (consisting of intermediate states), leading to a rather small surface tension. This physical picture is very similar to what is usually called a ''cluster spin glass,'' motivated by the observations made in Ref. 9 based on NMR experiments.

For a quantitative analysis we have to develop a theory for the bare surface tension σ_0 for the stripe glass. This differs from the theory of molecular liquids because of the long-range forces in the model. In what follows we give simple estimates for σ_0, based on a variational argument. There are two sources of the bare surface tension in Eq. (1), the gradient term and the long-range Coulomb term. Assuming a droplet configuration with locally ordered charge configuration

$$\varphi(r)=\varphi_0\cos(2\pi r/l_m)\tanh\left(\frac{r-R}{l_w}\right), \tag{52}$$

with droplet radius R and wall thickness l_w. In order to make progress, we assume that the thin-wall limit $l_w\ll R$ applies and find for the gradient term

$$E_s^{(1)}=4\pi\varphi_0^2l_w^{-2}\int_{R-l_w/2}^{R+l_w/2}r^2dr\simeq4\pi\varphi_0^2l_w^{-1}R^2 \tag{53}$$

and for the long-range Coulomb term

$$E_s^{(2)}\simeq4\pi\varphi_0^2l_m^{-1}R^2. \tag{54}$$

For larger values of the frustration parameter Q, l_w is estimated by the largest length scale of the problem (except R of course) which should correspond to the lowest energy of the droplet wall. This gives $l_w=\xi$. Alternatively, for smaller values of Q the surface tension is dominated by the contribution of the Coulomb term and we find

$$\sigma_0=4\pi\varphi_0^2l_m^{-1}.$$

From the same variational argument we find $\varphi_0^2=(1/u)Q^{1/2}$, which gives, together with $l_m\simeq2\pi Q^{1/4}$, the result $\sigma_0\simeq(2/u)Q^{3/4}$. Thus, if the frustration parameter decreases, the barrier height between different metastable states disappears. Even though the number of metastable states and thus $dS_c/dT|_{T_K}$ decreases for decreasing Q, the surface tension term dominates and it follows that

$$D(Q\to0)\to0. \tag{55}$$

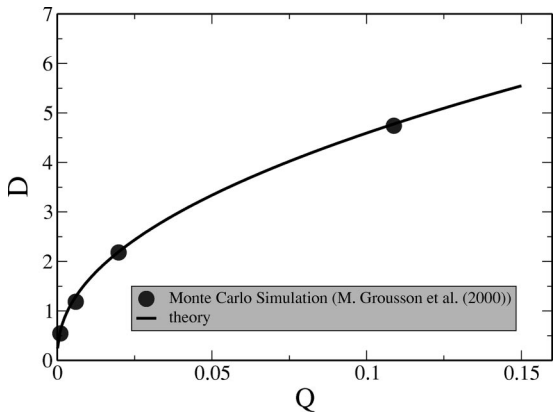

FIG. 8. Comparison of D with the results obtained in Monte Carlo simulations of the lattice version of Eq. (1) by Grousson *et al.* (Ref. 33).

The fragility parameter does not vanish according to a power law, mostly because $T_A - T_K$, which enters $dS_c/dT|_{T_K} \simeq S_c(T_A)/(T_A - T_K)$ has logarithmic behavior as $Q \to 0$. Essentially, D vanishes with Q similar to a square root. In Fig. 8 we compare $D(Q)$ with the results obtained in Monte Carlo simulations of the lattice version of Eq. (1) by Grousson *et al.*[33] Here we multiplied the result from Eq. (51) by an overall prefactor, leading to a very good agreement between our analytical theory and the numerical results of Ref. 33. Since the calculations in Ref. 33 are performed for a lattice version of Eq. (1), the actual T dependence of the correlation length differs from ours. Correspondingly the absolute magnitudes of T_K, which enters in Eq. (51), are different. For this reason we do not expect the absolute magnitude of D, but solely its Q dependence to agree in both approaches.

V. CONCLUSIONS

Glasses are typical examples of systems of many interacting particles that have a tendency to self-organize into mesoscopic structures. In this paper we studied the slow activated dynamics of charge inhomogeneities in doped Mott insulators. We developed an analytical approach which enabled us to identify the underlying physical mechanism for glassiness in a uniformly frustrated system. We showed that when the charge correlations are sufficiently strong, specifically if $\xi/l_m > 2$, the stripe-liquid–stripe-solid transition can become kinematically inaccessible because the system undergoes a glass transition, driven by the emergence of an extensive configurational entropy. We demonstrated that at this point a Lindemann length λ emerges, which is a length scale over which imperfections of the stripe pattern manage to wander. Finally, we apply our results to the scenario of Ref. 24 to calculate the characteristic relaxation time of the nonequilibrium state. We concluded that the charge fluctuations in doped Mott insulators have a tendency to self-organize into droplets of metastable states, distinguished by the packing of stripes with different orientation and the arrangement of defects. These droplets relax according to a Vogel-Fulcher law, characteristic of structural glasses. We further compare our results with the doping dependence of T_K, as deduced from experiment in Ref. 19, and show that it is properly described within our theory.

ACKNOWLEDGMENTS

We are grateful to N. Curro, P.C. Hammel, S. A. Kivelson, Z. Nussinov, D. Pines, and G. Tarjus for useful discussions and G. Tarjus for communicating the results of their Monte Carlo simulations. This research was supported by an award from Research Corporation (J.S.), the Institute for Complex Adaptive Matter, the Ames Laboratory, operated for the U.S. Department of Energy by Iowa State University under Contract No. W-7405-Eng-82 (H.W. and J.S.), and National Science Foundation Grant No. CHE-9530680 (P.G.W.). H.W. also acknowledges support from FAPESP.

APPENDIX A: SELF-CONSISTENT SCREENING APPROXIMATION

In this appendix we summarize the self-consistent screening approximation which was the basis of the numerical investigation of stripe glasses in Ref. 16 and which is the framework in which we determined the diagonal and off-diagonal element in replica space of the self-energy, leading in particular to Eq. (35). The details of the calculation of Eq. (35) are then given in Appendix B.

Equation (24) has a formal similarity to the action of the random-field Ising model, obtained within the conventional replica approach, which allows us to use techniques, developed for this model.[46] Introducing an N-component version of Eq. (1) with field $\varphi = (\varphi_1, \ldots, \varphi_N)$ and coupling constant $u = u_0/N$ with fixed u_0 we use a self-consistent screening approximation,[47] which is exact up to order $1/N$. At the end we perform the limit $N = 1$. The applicability of this approximation is supported by the strong indications for a nonsingular large-N limit of Eq. (1), as discussed in Ref. 28.

Before we discuss the self-consistent screening approximation, it is useful to summarize a few properties of matrices in replica space with structure similar to Eq. (26). Introducing a matrix $\mathbf{E}$ such that $\mathbf{E}_{ab} = 1$ and the unit matrix $\mathbf{1}$, it is easy to see that the product of any two $m \times m$ matrices with structure

$$\mathbf{A} = a_1 \mathbf{1} + a_2 \mathbf{E}, \tag{A1}$$

is given by

$$\mathbf{AB} = (a_1 b_1)\mathbf{1} + (a_1 b_2 + a_2 b_1 + m a_2 b_2)\mathbf{E}.$$

This leads to

$$\mathbf{A}^{-1} = \frac{1}{a_1}\mathbf{1} - \frac{a_2}{a_1(a_1 + m a_2)}\mathbf{E} \tag{A2}$$

for the inverse of $\mathbf{A}$. This property was used for the derivation of Eqs. (27) and (28) and will be used below.

The self-consistent screening approximation is described by the set of Feynman diagrams shown in Fig. 9. The self-energy, beyond the Hartree term which is diagonal in the replica index and was already taken into account in the bare propagator [Eq. (12)], is given by

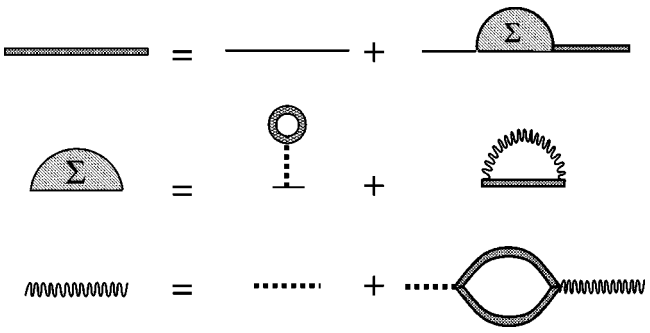

FIG. 9. Diagrams for the self-consistent screening approximation.

$$\Sigma_{ab}(\mathbf{q}) = \frac{2}{N}\int \frac{d^3p}{(2\pi)^3}\mathcal{D}_{ab}(\mathbf{p})\mathcal{G}_{ab}(\mathbf{p}+\mathbf{q}), \tag{A3}$$

where

$$\mathcal{D}(\mathbf{p}) = [v_0^{-1} + \Pi(\mathbf{p})]^{-1} \tag{A4}$$

is determined self-consistently by the polarization function

$$\Pi_{ab}(\mathbf{p}) = \int \frac{d^3q}{(2\pi)^3}\,\mathcal{G}_{ab}(\mathbf{q}+\mathbf{p})\mathcal{G}_{ba}(\mathbf{q}). \tag{A5}$$

In the above set of equations the p integration has to be cut off at $|\mathbf{p}| = \Lambda$ and the temperature T and the coupling constant u_0 occur only in the combination $v_0 = u_0 T$. The ansatz (26) for the Green's function implies an analogous structure for $\Sigma_{ab}(\mathbf{q})$ and $\Pi_{ab}(\mathbf{q})$ in replica space. Inserting this ansatz into $\Pi_{ab}(\mathbf{p})$ gives

$$\Pi = (\Pi_{\mathcal{G}} - \Pi_{\mathcal{F}})\mathbf{1} + \Pi_{\mathcal{F}}\mathbf{E}, \tag{A6}$$

where the diagonal and off-diagonal elements of the polarization function are

$$\Pi_{\mathcal{G}}(\mathbf{p}) = \int \frac{d^3q}{(2\pi)^3}\,\mathcal{G}(\mathbf{q}+\mathbf{p})\mathcal{G}(\mathbf{q}),$$

$$\Pi_{\mathcal{F}}(\mathbf{p}) = \int \frac{d^3q}{(2\pi)^3}\mathcal{F}(\mathbf{q}+\mathbf{p})\mathcal{F}(\mathbf{q}). \tag{A7}$$

Using the rule (A2), it is now straightforward to determine $\mathcal{D}_{ab}(\mathbf{p})$ which leads, in the limit $m \to 1$, to

$$\mathcal{D} = (\mathcal{D}_{\mathcal{G}} - \mathcal{D}_{\mathcal{F}})\mathbf{1} + \mathcal{D}_{\mathcal{F}}\mathbf{E}, \tag{A8}$$

where

$$\mathcal{D}_{\mathcal{G}}(\mathbf{p}) = [v_0^{-1} + \Pi_{\mathcal{G}}(\mathbf{p})]^{-1} \tag{A9}$$

and

$$\mathcal{D}_{\mathcal{F}}(\mathbf{p}) = -\frac{\Pi_{\mathcal{F}}(\mathbf{p})\mathcal{D}_{\mathcal{G}}^2(\mathbf{p})}{1 - \Pi_{\mathcal{F}}(\mathbf{p})\mathcal{D}_{\mathcal{G}}(\mathbf{p})}. \tag{A10}$$

Analogously, inserting the above equations into Eq. (A3) we get for the self-energies

$$\Sigma = (\Sigma_{\mathcal{G}} - \Sigma_{\mathcal{F}})\mathbf{1} + \Sigma_{\mathcal{F}}\mathbf{E},$$

where

$$\Sigma_{\mathcal{G}}(\mathbf{q}) = \frac{2}{N}\int \frac{d^3p}{(2\pi)^3}\mathcal{D}_{\mathcal{G}}(\mathbf{p})\mathcal{G}(\mathbf{p}+\mathbf{q}) \tag{A11}$$

and

$$\Sigma_{\mathcal{F}}(\mathbf{q}) = \frac{2}{N}\int \frac{d^3p}{(2\pi)^3}\mathcal{D}_{\mathcal{F}}(\mathbf{p})\mathcal{F}(\mathbf{p}+\mathbf{q}).$$

The set of equations is closed by the Dyson equation (25),

$$\mathcal{G}^{-1}(\mathbf{q})|_{ab} = [\mathcal{G}_0^{-1}(\mathbf{q}) + \Sigma_{\mathcal{G}} - \Sigma_{\mathcal{F}}]\mathbf{1} + \Sigma_{\mathcal{F}}\mathbf{E}, \tag{A12}$$

which gives, according to Eq. (A2), in the limit $m \to 1$ Eqs. (27) and (28).

In Ref. 16 it was shown that this coupled set of equations gives $\Sigma_{\mathcal{F}}(\mathbf{q}) \neq 0$ below a characteristic temperature which was related to the occurrence of glassiness. In the next appendix we present an approximate analytical solution of this problem.

APPENDIX B: ANALYSIS OF THE SELF-ENERGY

In this appendix we give the main technical details for the calculation of the off-diagonal self-energy in replica space, $\Sigma_{\mathcal{F}}$. The diagonal self-energy $\Sigma_{\mathcal{G}}$, which turns out to be negligibly small compared to the leading mean-field terms, can be determined in a very similar fashion and was already analyzed in Refs. 28 and 48, $\Sigma_{\mathcal{F}}$ and $\Sigma_{\mathcal{G}}$ were calculated numerically within the self-consistent screening approximation in Ref. 16. The virtue of the analytical calculation presented here is that it is much more transparent. In all steps of this calculation we did check the reliability of our approximate analytical treatment by comparing it with the numerical results.

We start by calculating the polarization function $\Pi_{\mathcal{G}}(q)$:

$$\begin{aligned}\Pi_G(q) &= \int \frac{d^3p}{8\pi^3}\mathcal{G}_{\mathbf{p}}\mathcal{G}_{\mathbf{p}+\mathbf{q}} \\ &= \left\{ \tan^{-1}\left(\frac{q}{\varepsilon q_m}\right) + \frac{1}{2}\tan^{-1}\left(\frac{2q_m - q}{\varepsilon q_m}\right) \right. \\ &\quad \left. - \frac{1}{2}\tan^{-1}\left(\frac{2q_m + q}{\varepsilon q_m}\right)\right\}(8\pi q\varepsilon^2)^{-1} \\ &\simeq \begin{cases} \dfrac{1}{8\pi q_m \varepsilon^3}, & q < \dfrac{2\varepsilon q_m}{\pi}, \\ \dfrac{\Theta(2q_m - q)}{16 q \varepsilon^2}, & q > \dfrac{2\varepsilon q_m}{\pi}, \end{cases}\end{aligned}$$

where we used the approximate expression, (11) for the correlation function $\mathcal{G}(\mathbf{x})$. An analogous calculation for the off-diagonal polarization function $\Pi_{\mathcal{F}}(q)$ gives

$$\int \frac{d^3p}{8\pi^3}\mathcal{K}(\mathbf{p})\mathcal{K}(\mathbf{p}+\mathbf{q}) \simeq \begin{cases} \dfrac{1}{8\pi q_m \kappa^3}, & q<\dfrac{2\kappa q_m}{\pi}, \\ \dfrac{\Theta(2q_m-q)}{16\kappa^2 q}, & q>\dfrac{2\kappa q_m}{\pi}, \end{cases}$$

as well as

$$\int \frac{d^3p}{8\pi^3}\mathcal{G}(\mathbf{p})\mathcal{K}(\mathbf{p}+\mathbf{q}) \simeq \begin{cases} \dfrac{1}{8\pi q_m \kappa^3}, & q<\dfrac{\kappa+\varepsilon}{\pi}q_m, \\ \dfrac{\Theta(2q_m-q)}{16\kappa\varepsilon q}, & q>\dfrac{\kappa+\varepsilon}{\pi}q_m. \end{cases}$$

For $(\varepsilon,\kappa)q_m<q<2q_m$, we can use the approximate expressions

$$\Pi_{\mathcal{G}}(q)=\frac{1}{16q\varepsilon^2},$$

$$\Pi_{\mathcal{F}}(q)=\frac{1}{16q}\left(\frac{1}{\varepsilon}-\frac{1}{\kappa}\right)^2,$$

which gives

$$D_{\mathcal{G}}(q)=\frac{16q_m a}{1+\dfrac{q_m}{q}\dfrac{a}{\varepsilon^2}},$$

with dimensionless number $a=v_0/16q_m \lesssim 1$. Here a vanishes as $T\to 0$, but it always holds that $\varepsilon^2 \ll a$. Note that for the numerical solution in Ref. 16 it holds that $a\simeq 0.4$. Combining these results and using the fact that $\varepsilon^2/a \ll 1$, the product $D_{\mathcal{G}}(q)\Pi_{\mathcal{F}}(q)$ becomes momentum independent,

$$D_{\mathcal{G}}(q)\Pi_{\mathcal{F}}(q)\simeq\left(1-\frac{\varepsilon}{\kappa}\right)^2,$$

and, as a result, $D_{\mathcal{F}}(q)$ becomes proportional (by a factor smaller than 1 in magnitudes) to $D_{\mathcal{G}}(q)$:

$$D_{\mathcal{F}}(q)=\left[\frac{-D_{\mathcal{G}}(q)\Pi_{\mathcal{F}}(q)}{1-D_{\mathcal{G}}(q)\Pi_{\mathcal{F}}(q)}\right]D_{\mathcal{G}}(q) \tag{B1}$$

$$\simeq\left[\frac{-\left(1-\dfrac{\varepsilon}{\kappa}\right)^2}{1-\left(1-\dfrac{\varepsilon}{\kappa}\right)^2}\right]D_{\mathcal{G}}(q). \tag{B2}$$

We are now in the position to analyze the self-energy $\Sigma_{\mathcal{F}}$:

$$\Sigma_{\mathcal{F}}(\mathbf{q})=2\int\frac{d^3p}{8\pi^3}D_{\mathcal{F}}(\mathbf{q}+\mathbf{p})\mathcal{F}(\mathbf{p}). \tag{B3}$$

Since $D_{\mathcal{F}}(\mathbf{q})$ is only weakly momentum dependent, the same holds for $\Sigma_{\mathcal{F}}(\mathbf{q})$ and we can estimate it at the modulation vector. It follows with $t=\sqrt{2(1+\cos\theta)}$

$$\Sigma_{\mathcal{F}}(q_m)\simeq\int_0^2 t\,dt\,D_{\mathcal{F}}(q_m t)\int\frac{p^2dp}{4\pi^2}\mathcal{F}(p)$$

$$\simeq D_{\mathcal{F}}(q_m)\int\frac{p^2dp}{4\pi^2}\mathcal{F}(p). \tag{B4}$$

Using $\mathcal{F}(p)=\mathcal{G}(p)-\mathcal{K}(p)$ and

$$\int\frac{p^2dp}{8\pi^3}\mathcal{G}(p)=\frac{1}{2\pi^2}\left(\frac{\pi q_m}{2\varepsilon}+\Lambda\right)$$

as well as

$$\int\frac{p^2dp}{8\pi^3}\mathcal{K}(p)=\frac{1}{2\pi^2}\left(\frac{\pi q_m}{2\kappa}+\Lambda\right),$$

we find

$$\Sigma_{\mathcal{F}}(q_m)=-\frac{8q_m^2\varepsilon^2}{\pi}\frac{\left(1-\dfrac{\varepsilon}{\kappa}\right)^2}{1-\left(1-\dfrac{\varepsilon}{\kappa}\right)^2}\left(\frac{1}{\varepsilon}-\frac{1}{\kappa}\right). \tag{B5}$$

Thus, we have determined the off-diagonal self-energy at the modulation wave vector as a function of the three essential length scales of the problem: $l_m=2\pi/q_m$, $\xi=2/\varepsilon q_m$, and $\lambda=\dfrac{2}{(\sqrt{\kappa^2-\varepsilon^2}q_m)}$. Note the dependence on the momentum cutoff, Λ, cancels, completely making this result robust against lattice corrections.

APPENDIX C: COMPARISON WITH THE FRUSTRATION-LIMITED DOMAIN SCENARIO

The possibility of glass formation of the model, Eq. (1), has been pointed out in Ref. 29. As discussed in this appendix, we disagree with the detailed argumentation of Ref. 29. However, the recognition that a model of the kind of Eq. (1) can potentially describe glass formation was a very important observation.

The aim of Ref. 29 was to present an alternative scenario for glassiness in structural glasses formed of undercooled molecular liquids. Though the microscopic justification of Eq. (1) for the description of structural glasses is at the least unresolved, one can yet, in principle, imagine that such long-range interactions are caused by a scenario like that based on icosahedral order which is frustrated by the lack of Euclidean curvature of the effective space.[5] In what follows we will solely consider Eq. (1) as a given model and leave aside whether it applies to stripe glasses in doped Mott insulators (as we claim) or to molecular liquids (as claimed in Ref. 29).

The main idea of Ref. 29 is that due to the frustrating interaction of Eq. (1) the system is broken up into ordered domains of size $R_D\sim\xi^{-1}Q^{-1/2}$ with ξ being the correlation length that controls the fluctuations inside ordered domains. Furthermore, $\xi\ll R_D$ is assumed. Within each domain the ordering essentially corresponds to the one of a finite $Q=0$ system (not of a system with stripes as in our entropic drop-

let picture). Since, for $Q=0$, ξ diverges at the critical point T_c^0, the avoided frustration scenario suggests that for $Q>0$, $\xi(T)$ still has a peak close to T_c^0, only rounded due to the frustration. It is then argued that there is a relaxation rate τ^{-1} due to the reorganization of domains which obeys an Arrhenius form

$$\tau^{-1} \propto e^{-\Delta F(R_D)/T}, \tag{C1}$$

where $\Delta F(R_D) \sim T_c^0 (R_D/\xi)^2$ is the activation energy of the domain. Finally, it is asserted that the divergence in the viscosity of the system at low temperatures is determined by $\eta \propto \tau$.

We disagree with this picture. As shown below, the scale R_D, which signals the relevance of the long-range interaction, can easily be identified as the Debye screening length of charged particles of size ξ with the expected charge density. Even when the Debye picture applies, we find it hard to understand how conventional screening can lead to a dynamics which is dominated by the activated reorganization of screening clouds and where the natural Langevin description gives a fast relaxation. When $\xi \ll R_D$ there are many short-wavelength excitations of weakly coupled charges and the system should rather behave as a high-temperature plasma than as a glass. In addition, for $N \to \infty$ it was shown in Ref. 28 that Debye screening occurs only at temperatures $T > T_c^0$. At low temperatures modulated structures result which lead to the formation of well-correlated stripes as $\xi > l_m$. Here $\xi(T)$ does not exhibit a maximum at a temperature comparable to T_c^0 but keeps growing until either a stripe solid or a stripe glass is formed.

We now show that the scale $R_D \sim \xi^{-1} Q^{-1/2}$ is the Debye screening length of charged particles of size ξ. We perform a coarse graining of the system into regions of linear size ξ centered around positions $\mathbf{X}_i$. Then Eq. (1) becomes

$$\mathcal{H} = \sum_i \mathcal{H}_i + \sum_{i>j} \frac{q_i q_j}{|\mathbf{X}_i - \mathbf{X}_j|}, \tag{C2}$$

where

$$\mathcal{H}_i \sim \frac{1}{2} \int_{\xi^3} d^3x \left\{ r_0 \varphi(\mathbf{x})^2 + [\nabla \varphi(\mathbf{x})]^2 + \frac{u}{2} \varphi(\mathbf{x})^4 \right\} \tag{C3}$$

and charges

$$q_i \simeq \sqrt{\frac{Q}{8\pi}} \int_\xi d^3x \, \varphi(\mathbf{x}) \propto \sqrt{Q} \xi^{5/2}.$$

In the last step we assumed that within the volume $\propto \xi^3$ the system is essentially ordered and used $\varphi \propto \xi^{-\beta/\nu}$, with the critical exponents $\beta = \frac{1}{2}$ and $\nu = (d-2)^{-1}$, obtained within the large N approximation, for $d=3$.[49]

The usual analysis of Eq. (C2) within the Debye approximation, i.e., solving the Poisson equation with induced charges distributed with Boltzmann weight, gives the Debye screening length

$$l_D^{-2} = \frac{2\pi q_i^2}{T} n,$$

where n is the density of charges, here given by $n \simeq \xi^{-3}$. This finally gives

$$l_D \sim Q^{-1/2} \xi^{-1},$$

which is precisely the length R_D proposed in Ref. 28.

In summary, it is unclear why Debye screening should cause a breakup of the system into ordered domains of size $R_D = l_D$ (remember $\xi \ll l_D$) and a slow activated dynamics of such domains, necessary to obtain large viscosities. Second, for the scenario of Ref. 29 to work, one also has to assume that the correlation length decreases at low temperature and that Debye theory still applies. The actual analysis of Eq. (1) for $N \to \infty$ does not show both assumptions to be justified.[28] However, it is interesting that for $N < \infty$ the emergence of a Josephson length scale at low temperatures[28] might give rise to a competition of physics on two distinct length scales which then, in principle, could lead to a new long-time relaxation along the lines of the frustration-limited domain approach.[50] It is interesting to explore the relationship of this new scenario to our replica-based theory.

Finally, it is worth pointing out that the entropic droplets discussed in this paper are qualitatively different from the domains introduced in the approach of Ref. 29. Whereas the latter correspond to thermodynamically stable configurations, similar to domains in ferromagnets caused by the long-ranged dipole-dipole interaction, our entropic droplets are formed by the various metastable states. Transitions between different droplets are caused by a gain of entropy of a system in what would be an otherwise frozen nonequilibrium state.

[1] T. Garel and S. Doniach, Phys. Rev. B **26**, 325 (1982).
[2] R. Allenspach and A. Bischof, Phys. Rev. Lett. **69**, 3385 (1992).
[3] P. G. de Gennes and C. Taupin, J. Phys. Chem. **86**, 2294 (1982).
[4] W. M. Gelbart and A. Ben Shaul, J. Phys. Chem. **86**, 2294 (1982).
[5] D. R. Nelson, J. Non-Cryst. Solids **75**, 77 (1985); S. Sachdev and D. R. Nelson, Phys. Rev. B **32**, 4592 (1985).
[6] J. H. Cho, F. C. Chou, and D. C. Johnston, Phys. Rev. Lett. **70**, 222 (1993).
[7] J. M. Tranquada, B. J. Sternlieb, J. D. Axe, Y. Nakamura, and S. Uchida, Nature (London) **375**, 561 (1995).
[8] V. J. Emery and S. A. Kivelson, Physica C **209**, 597 (1993).
[9] J. H. Cho, F. Borsa, D. C. Johnston, and D. R. Torgeson, Phys. Rev. B **46**, 3179 (1992).
[10] S. H. Lee and S. W. Cheong, Phys. Rev. Lett. **79**, 2514 (1997).
[11] J. M. Tranquada, N. Ichikawa, and S. Uchida, Phys. Rev. B **59**, 14712 (1999).
[12] M.-H. Julien, F. Borsa, P. Carretta, M. Horvatic, C. Berthier, and C. T. Lin, Phys. Rev. Lett. **83**, 604 (1999).
[13] A. W. Hunt, P. M. Singer, K. R. Thurber, and T. Imai, Phys. Rev. Lett. **82**, 4300 (1999).
[14] N. J. Curro, P. C. Hammel, B. J. Suh, M. Hücker, B. Büchner, U. Ammerahl, and A. Revcolevschi, Phys. Rev. Lett. **85**, 642

(2000).
[15] J. Haase, C. P. Slichter, R. Stern, C. T. Milling, and D. G. Hinks, Physica C **341**, 1727 (2000).
[16] J. Schmalian and P. G. Wolynes, Phys. Rev. Lett. **85**, 836 (2000).
[17] J. Schmalian, H. Westfahl, Jr., and P. G. Wolynes, Int. J. Mod. Phys. B (to be published).
[18] B. P. Stojkovic, Z. G. Yu, A. R. Bishop, A. H. Castro-Neto, and N. Grønbech-Jensen, Phys. Rev. Lett. **82**, 4679 (1999); cond-mat/9911380 (unpublished).
[19] R. S. Markiewicz, F. Cordero, A. Paolone, and R. Cantelli, Phys. Rev. B **64**, 054409 (2001).
[20] S. Wakimoto, G. Shirane, Y. Endoh, K. Hirota, S. Ueki, K. Yamada, R. J. Birgeneau, M. A. Kastner, Y. S. Lee, P. M. Gehring, and S. H. Lee, Phys. Rev. B **60**, 769 (1999).
[21] A. Campana, R. Cantelli, F. Cordero, M. Corti, and A. Rigamonti, Int. J. Mod. Phys. B **14**, 2749 (2000).
[22] Ch. Niedermeyer, C. Bernhard, T. Blasius, A. Golnik, A. Moodenbaugh, and J. I. Budnik, Phys. Rev. Lett. **80**, 3843 (1998).
[23] S. Wakimoto, S. Ueki, Y. Endoh, and Y. Yamada, Phys. Rev. B **62**, 3547 (2000).
[24] T. R. Kirkpatrick and D. Thirumalai, and P. G. Wolynes, Phys. Rev. A **40**, 1045 (1989); T. R. Kirkpatrick and P. G. Wolynes, Phys. Rev. B **36**, 8552 (1987); Phys. Rev. A **35**, 3072 (1987); T. R. Kirkpatrick and D. Thirumalai, Phys. Rev. Lett. **58**, 2091 (1987).
[25] J. P. Stoessel and P. G. Wolynes, J. Chem. Phys. **80**, 4502 (1984).
[26] R. Monnason, Phys. Rev. Lett. **75**, 2875 (1995).
[27] M. Mezard and G. Parisi, Phys. Rev. Lett. **82**, 747 (1999).
[28] Z. Nussinov, J. Rudnick, S. A. Kivelson, and L. N. Chayes, Phys. Rev. Lett. **83**, 472 (1999).
[29] D. Kivelson, S. A. Kivelson, X. Zhao, Z. Nussinov, and G. Tarjus, Physica A **219**, 27 (1995).
[30] L. Chayes, V. J. Emery, S. A. Kivelson, Z. Nussinov, and G. Tarjus, Physica A **225**, 129 (1996).
[31] S. A. Brazovskii, Sov. Phys. JETP **41**, 85 (1975).
[32] A. W. Kauzman, Chem. Rev. **43**, 219 (1948).
[33] M. Grousson, G. Tarjus, and P. Viot, Phys. Rev. Lett. **86**, 3455 (2001).
[34] K. Yamada, C. H. Lee, K. Kurahashi, J. Wada, S. Wakimoto, S. Ueki, H. Kimura, Y. Endoh, S. Hosoya, G. Shirane, R. J. Birgeneau, M. Greven, M. A. Kastner, and Y. J. Kim, Phys. Rev. B **57**, 6165 (1998).
[35] P. Chandra, L. B. Ioffe, and D. Sherrington, Phys. Rev. Lett. **75**, 713 (1995); Phys. Rev. B **58**, R14 669 (1998).
[36] S. Franz and J. Hertz, Phys. Rev. Lett. **74**, 2114 (1995).
[37] L. Cugliandolo, J. Kurchan, R. Monasson, and G. Parisi, J. Phys. A **29**, 1347 (1996).
[38] J.-P. Bouchaud, L. Cugliandolo, J. Kurchan, and M. Mezard, Physica A **226**, 243 (1996).
[39] H. Westfahl, Jr., J. Schmalian, and P. G. Wolynes (unpublished).
[40] A. Crisanti and H.-J. Sommers, J. Phys. I **5**, 805 (1995).
[41] J. Zinn-Justin, *Quantum Field Theory and Critical Phenomena* (Clarendon Press, Oxford, 1989).
[42] L. Cugliandolo and J. Kurchan, Phys. Rev. Lett. **71**, 1 (1993).
[43] J. Villain, J. Phys. (Paris) **46**, 1843 (1985); Phys. Rev. Lett. **52**, 1543 (1984).
[44] X. Xia and P. G. Wolynes, Proc. Nat'l. Acad. Sci. USA **97**, 2990 (2000).
[45] X. Xia and P. G. Wolynes, J. Phys. Chem. B **105**, 6570 (2001).
[46] M. Mezard and A. P. Young, Europhys. Lett. **18**, 653 (1992).
[47] A. J. Bray, Phys. Rev. Lett. **32**, 1413 (1974).
[48] Z. Nussinov, Ph.D. thesis, University of California at Los Angeles, 2000.
[49] S.-K. Ma, *Modern Theory of Critical Phenomena* (Benjamin, Reading, MA, 1976).
[50] S. A. Kivelson (private communication).